

The response of tropical tropospheric ozone to ENSO

L. D. Oman,¹ J. R. Ziemke,^{1,2} A. R. Douglass,¹ D. W. Waugh,³ C. Lang,³
J. M. Rodriguez,¹ and J. E. Nielsen^{1,4}

Received 19 April 2011; revised 2 June 2011; accepted 5 June 2011; published 13 July 2011.

[1] We have successfully reproduced the Ozone ENSO Index (OEI) in the Goddard Earth Observing System (GEOS) chemistry-climate model (CCM) forced by observed sea surface temperatures over a 25-year period. The vertical ozone response to ENSO is consistent with changes in the Walker circulation. We derive the sensitivity of simulated ozone to ENSO variations using linear regression analysis. The western Pacific and Indian Ocean region shows similar positive ozone sensitivities from the surface to the upper troposphere, in response to positive anomalies in the Niño 3.4 Index. The eastern and central Pacific region shows negative sensitivities with the largest sensitivity in the upper troposphere. This vertical response compares well with that derived from SHADOZ ozonesondes in each region. The OEI reveals a response of tropospheric ozone to circulation change that is nearly independent of changes in emissions and thus it is potentially useful in chemistry-climate model evaluation. **Citation:** Oman, L. D., J. R. Ziemke, A. R. Douglass, D. W. Waugh, C. Lang, J. M. Rodriguez, and J. E. Nielsen (2011), The response of tropical tropospheric ozone to ENSO, *Geophys. Res. Lett.*, 38, L13706, doi:10.1029/2011GL047865.

1. Introduction

[2] The El Niño–Southern Oscillation (ENSO) is the dominant mode of tropical variability on interannual timescales [Philander, 1989]. ENSO has been long known to cause significant perturbations to the coupled oceanic and atmospheric circulations [Bjerknes, 1969; Enfield, 1989]. Changes in sea surface temperatures in the Pacific Ocean can notably impact the Walker Circulation, displacing areas of convective activity, and have also been shown to dominate the interannual variability of the Hadley cell [Quan et al., 2004]. These changes in circulation cause changes in the temperature and moisture fields across the tropical Pacific, and influence the constituent distributions in the troposphere [Chandra et al., 1998, 2002, 2009; Sudo and Takahashi, 2001; Ziemke and Chandra, 2003; Zeng and Pyle, 2005; Doherty et al., 2006; Lee et al., 2010; Randel and Thompson, 2011] and in the stratosphere [Randel and Cobb, 1994].

[3] Ziemke et al. [2010] used tropospheric column ozone (TCO) measurements to show that the ENSO related response of tropospheric ozone over the western and eastern Pacific

dominated interannual variability. The ENSO impact is so clearly seen in tropospheric ozone columns that an Ozone ENSO Index (OEI) that largely mimics the Niño 3.4 Index is formed by subtracting the eastern and central tropical Pacific region TCO (15°S–15°N, 110°W–180°W) from the western tropical Pacific-Indian Ocean region (15°S–15°N, 70°E–140°E), removing the seasonal cycle and smoothing with a 3-month running average. Ziemke et al. [2010] suggested that chemistry-climate models forced with observed sea surface temperatures should reproduce this observed pattern in tropospheric ozone. Here we will show that in the GEOS CCM tropical tropospheric ozone responds to the perturbation in atmospheric dynamics that is due to the ENSO signature in tropical SSTs. In addition, we use the Southern Hemisphere Additional Ozonesondes (SHADOZ) measurements to evaluate the vertical structure of the simulated response to ENSO.

2. Model Simulation and Measurements

[4] We examine the response of simulated tropospheric ozone to the observed sea surface temperature changes using the Goddard Earth Observing System (GEOS) version 5 general circulation model [Rienecker et al., 2008] coupled to the comprehensive Global Modeling Initiative (GMI) stratosphere-troposphere chemical mechanism [Duncan et al., 2007; Strahan et al., 2007]. The GMI combined stratosphere-troposphere chemistry mechanism includes 117 species, 322 chemical reactions, and 81 photolysis reactions. Integration of the chemical mass balance equations use the SMVGEAR II algorithm described by Jacobson [1995]. The mechanism includes a detailed description of O₃-NO_x-hydrocarbon chemistry necessary for the troposphere [Bey et al., 2001], with more recent updates described by Duncan et al. [2007]. The simulation used in this study was forced with observed sea surface temperatures and sea ice concentrations from 1985 to 2009 [Rayner et al. [2003], updated on a monthly basis), but the seasonally-varying mixing ratio boundary conditions and emissions for trace gases are for 2005 conditions. The simulation produces the variability in constituent distributions due to sea surface temperature changes that we evaluate here.

[5] A record of TCO for the 2005–2010 period was derived from the combination of NASA's Aura satellite Ozone Monitoring Instrument (OMI) and the Microwave Limb Sounder (MLS) using the method described by Ziemke et al. [2006]. These TCO values extend the time series developed using Nimbus 7 TOMS, Earth Probe TOMS and NOAA SBUV. The TCO measurements for 2005–2010 are used in Figure 1a. A complete description of the methods used to construct the OEI is given by Ziemke et al. [2010]. Here we use the index derived from TCO measurements for 1985–2009 to match the simulation. The OEI time series begins in 1979 and is updated periodically. The data can be obtained

¹NASA Goddard Space Flight Center, Greenbelt, Maryland, USA.

²GEST, University of Maryland, Baltimore County, Baltimore, Maryland, USA.

³Department of Earth and Planetary Science, Johns Hopkins University, Baltimore, Maryland, USA.

⁴Science Systems and Applications Inc., Lanham, Maryland, USA.

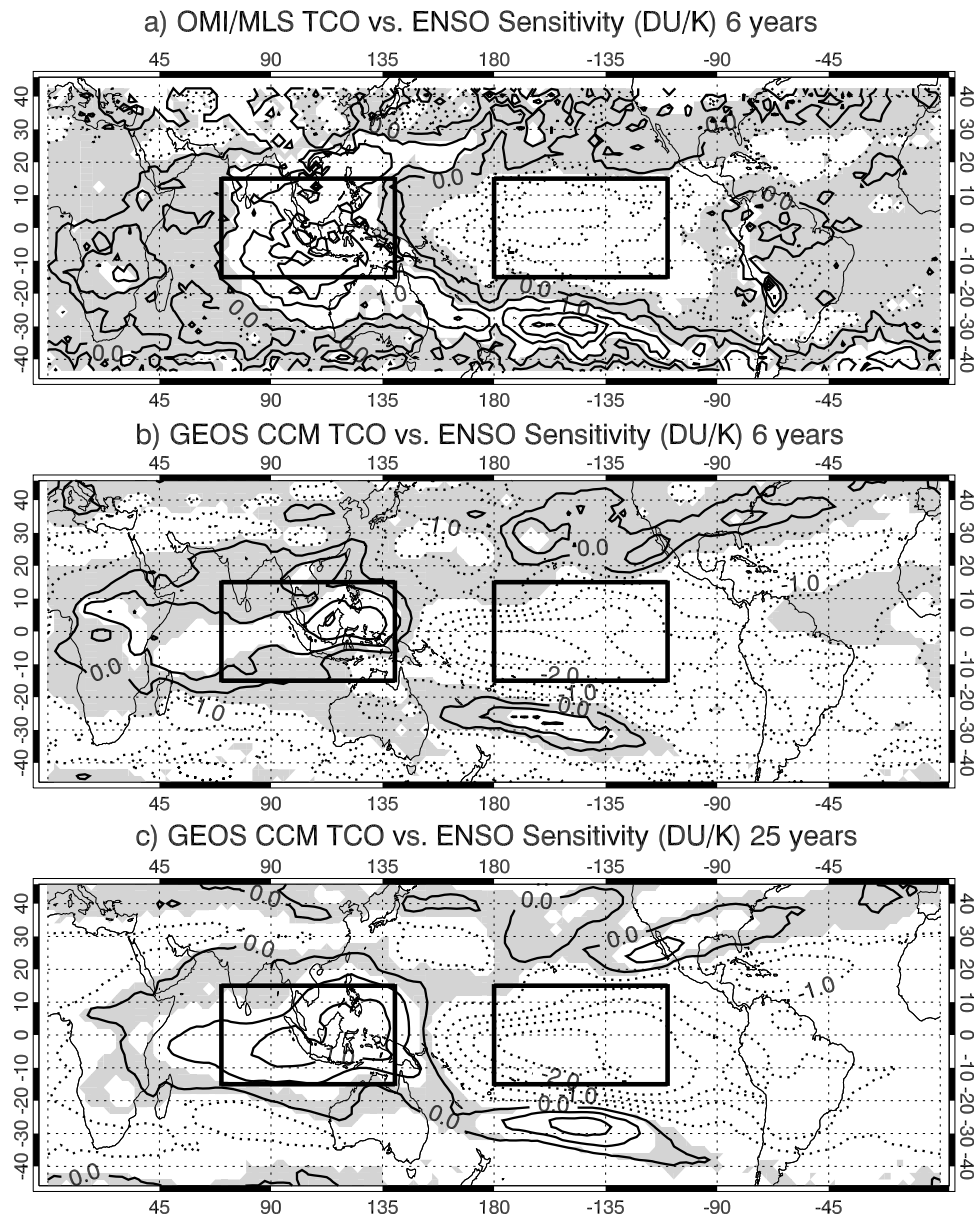


Figure 1. Comparison of the tropospheric column ozone sensitivity (DU/K) to the Niño 3.4 Index for (a) 6 years of MLS/OMI measurements, (b) 6 years of GEOS CCM simulation, (c) 25 years of GEOS CCM simulation. Shaded regions are not significant at the 95% level. The black rectangles show two regions used in calculating the Ozone ENSO Index.

from the Goddard tropospheric ozone website at <http://toms.gsfc.nasa.gov>.

[6] We use ozonesonde measurements from five SHADOZ stations [Thompson *et al.*, 2003] (<http://croc.gsfc.nasa.gov/shadoz>): two in the western region (Java and Kuala Lumpur) and three in the eastern region (American Samoa, Hilo, and San Cristobal). The data for Watukosek, Java (7.6°S, 112.7°E), Kuala Lumpur, Malaysia (2.7°N, 101.7°E), Pago Pago, American Samoa (14.2°S, 170.6°W), and Hilo, Hawaii (19.4°N, 155.0°W) cover the 1998 to 2009 time period, whereas the San Cristobal (0.9°S, 89.6°W) record is slightly shorter, covering 1998 to 2008.

[7] We used the ENSO index based on the Niño 3.4 region and available from the NOAA sea-surface temperature

website (<http://www.cpc.ncep.noaa.gov/data/indices/>), also used by Ziemke *et al.* [2010].

3. Results and Discussion

[8] Ziemke *et al.* [2010] used a combination of satellite observations and simulations to show that the observed tropical longitudinal structure in total column ozone was due almost entirely to structure in the TCO. They identified a dipole in tropical TCO between the western Pacific-Indian Ocean region and eastern and central Pacific region (15°S–15°N, 70°E–140°E, and 15°S–15°N, 110°W–180°W, respectively). The difference between the mean TCO in these two regions, shown as black rectangles on Figure 1, is called the Ozone ENSO Index (OEI). Also shown in Figure 1 is the TCO response to

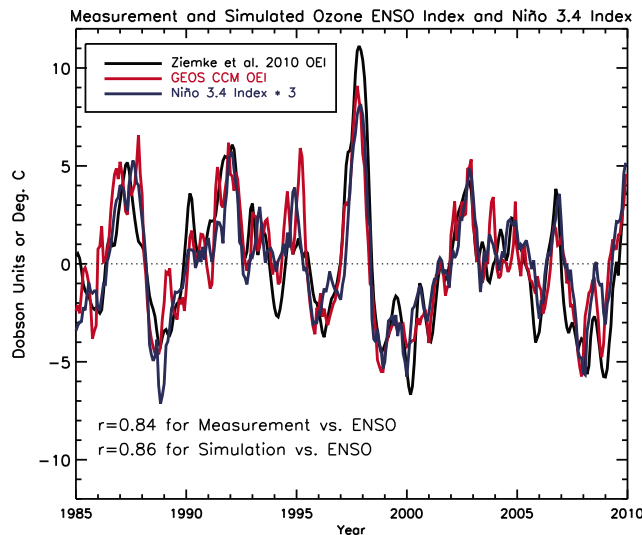


Figure 2. Comparison of GEOS CCM simulation and Ziemke *et al.*'s [2010] measurement derived Ozone ENSO Index (OEI) with Niño 3.4 Index (multiplied by 3) for the 1985 to 2009 time period.

the Niño 3.4 Index computed using linear regression analysis for both measurements and the GEOS chemistry-climate model (CCM) simulation. Regression of the TCO against Niño 3.4 Index yields a sensitivity coefficient or slope (DU/K) that represents the TCO change congruent with a 1 K increase in the Niño 3.4 Index. For reference, a typical El Niño/La Niña cycle represents about a 3 K range with about a 5 K range for a more extreme cycle. OMI/MLS derived TCO measurements [Ziemke *et al.*, 2006] for the 6 years covering 2005 to 2010 are used to calculate the sensitivity coefficient (DU/K) in Figure 1a. Significant positive TCO sensitivities are located throughout the western region with significant negative TCO sensitivities over the eastern region. Shaded regions show sensitivities that are not significant at the 95% level taking into account any autocorrelation of the residual. Figure 1b shows a similar 6-year period (in this case 2004 to 2009) from GEOS CCM simulated TCO. The overall pattern is similar to that derived from OMI/MLS TCO with a slightly negative offset in the simulation. Over the Indonesian region, the meridional extent of the positive anomalies is smaller in Figure 1b than 1a, which could partially be due to the short record. Also, shown (Figure 1c) is the sensitivity calculated using 25 years of the simulation (from 1985 to 2009). Another significant feature that appears in both measurements and simulation is positive TCO sensitivities in the central Pacific Ocean near 30°S.

[9] The OEI is the difference between the western region average monthly TCO and that computed for the eastern region. The deseasonalized time series of OEI, smoothed with a 3-month running average, is shown in Figure 2 for the measurements (black curve) and simulation (red curve). The Niño 3.4 Index multiplied by 3 is shown as the blue curve. There is excellent agreement between all three time series: The correlation of the measurement derived OEI with ENSO is 0.84 and that of the simulation derived OEI with ENSO is 0.86. During El Niño, the positive phase of ENSO, the OEI anomaly is positive, corresponding to increased

ozone over the western region and decreased ozone over the eastern region. This can be most clearly seen during the very strong 1997–1998 El Niño with an anomaly of 9 DU for OEI obtained from simulated tropospheric ozone columns compared with 11 DU from observations.

[10] The correspondence of observed and simulated OEI prompted us to examine the vertical structure of the dynamically driven ozone changes simulated with the GEOS CCM, again using linear regression analysis. Regression of the

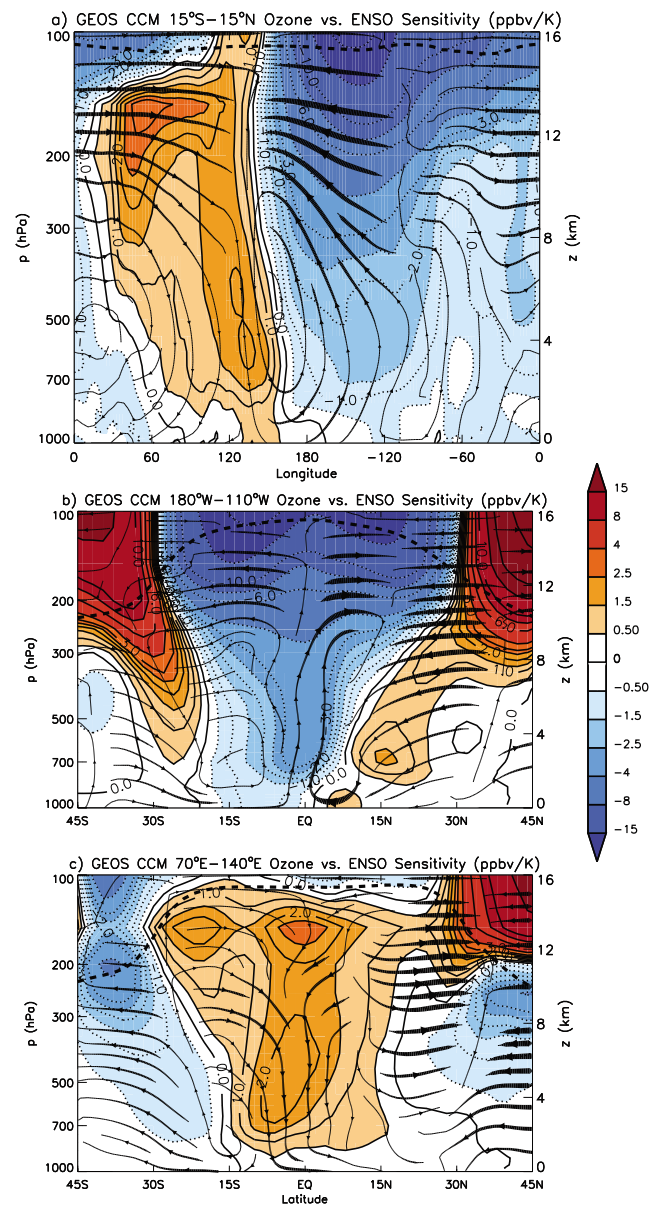


Figure 3. Sensitivity coefficient (ppbv/K) formed from linearly regressing deseasonalized (a) tropical (15°S–15°N), (b) eastern region (180°W–110°W), and (c) western region (70°E–140°E) average ozone against Niño 3.4 Index. Overlaid is the anomalous circulation shown by the streamfunction obtained by regressing the zonal wind and vertical velocity (Figure 2a), or meridional wind and vertical velocity (Figure 2b and 2c) against Niño 3.4 Index. The dashed black curve on all panels shows the mean model tropopause.

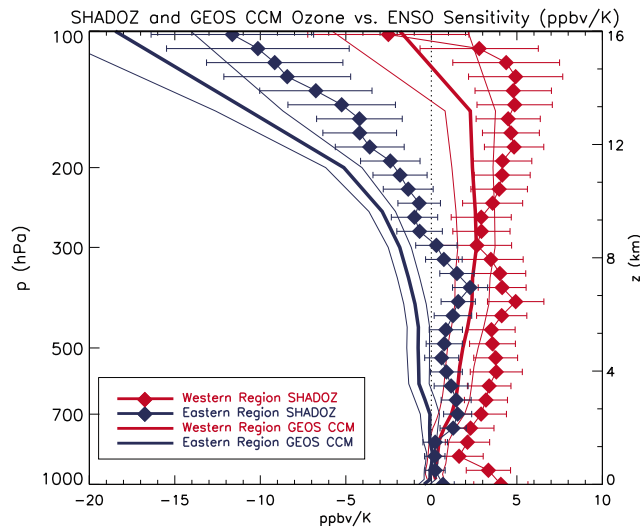


Figure 4. Vertical structure of ozone sensitivity (ppbv/K) to Niño 3.4 Index derived from SHADOZ ozonesondes over the western (red diamonds) and eastern (blue diamonds) regions of the tropical Pacific. GEOS CCM sensitivities sampled for the SHADOZ locations are shown as solid curves.

simulated tropical ozone field against the Niño 3.4 Index yields a sensitivity coefficient in ppbv/K. We average tropical tropospheric ozone between 15°S and 15°N and regress the deseasonalized ozone field with Niño 3.4 Index at each longitude and pressure level to construct Figure 3a. Since ENSO is known to produce a significant change in the Walker circulation, we overlay the anomaly in the streamfunction obtained by regressing the zonal wind and vertical velocity against the Niño 3.4 Index. The ozone and circulation anomalies generally have inflection points just to the west of the international date line, with lower ozone values and anomalous upwelling to the east and higher ozone values and anomalous downwelling to the west. The Walker circulation response is seen clearly in the streamfunction anomaly, which corresponds very well to the pattern of ozone sensitivity. Figure 3a shows that the simulated sensitivity of ozone to the Niño 3.4 Index in the western region as defined by Ziemke *et al.* [2010] is ~ 1 to 2 ppbv/K from the surface to the tropopause with relative maxima in the upper troposphere around 60°E and in the mid-troposphere around 130°E. Negative values of ozone sensitivity in the eastern region are largest in the upper troposphere approaching -15 ppbv/K near the tropopause.

[11] We also examine the latitude dependence of the ozone and circulation response in the two key regions identified by Ziemke *et al.* [2010]. The sensitivity coefficients (ppbv/K) formed from linearly regressing deseasonalized average ozone in the eastern region (180°W–110°W) and western region (70°E–140°E) against the Niño 3.4 Index for each latitude and altitude are given in Figures 3b and 3c respectively. Again we overlay the anomalous circulation shown by the streamfunction obtained this time by regressing the meridional wind and vertical velocity against the Niño 3.4 Index. The dashed black curve shows the mean model tropopause in each region. In the eastern region a stronger mean ascending branch of Walker circulation is seen near the equator. This simulated eastern region response of the cir-

ulation is consistent with the observed rawinsonde station data analyzed by Oort and Yienger [1996] and produces a corresponding tropospheric ozone response. The region of decreased ozone generally broadens in latitude as altitude increases with values from -3 ppbv/K in the equatorial mid-troposphere to -15 ppbv/K near the tropical tropopause. The positive ozone anomalies with increased tropical SSTs in the midlatitudes of Figure 3b could be consistent with increased stratosphere-troposphere exchange of ozone. Zeng and Pyle [2005] also found an increase in the stratosphere-troposphere exchange of ozone in their CCM simulation of the impact of ENSO. Other studies suggested observational evidence for this impact in observations above Colorado [Langford *et al.*, 1998; Langford, 1999]. The recent analysis of Voulgarakis *et al.* [2011] has also simulated enhanced stratosphere-troposphere exchange of ozone following the strong 1997–1998 El Niño event.

[12] Chandra *et al.* [1998] found that downward motion, suppressed convection, and a drier troposphere contribute to the ozone increase over the tropical western Pacific and Indonesian region. The combination of downward motion and suppressed convection bring ozone produced in the upper troposphere down [Sudo and Takahashi, 2001], and reduce the upward transport of low ozone air over ocean surfaces, increasing ozone values in the low to mid troposphere. Additionally, the drier troposphere increases the chemical lifetime of ozone, which also acts to increase tropospheric ozone concentrations [Kley *et al.*, 1996]. These results are consistent with the GEOS CCM simulation and are shown in Figure 3c by the anomalous downward component in the circulation.

[13] We evaluate the simulated vertical ozone response to ENSO using data collected by the SHADOZ network [Thompson *et al.*, 2003]. There are SHADOZ stations in and around the two key regions shown by Ziemke *et al.* [2010]. In Figure 4 we compare the simulated ENSO related vertical ozone sensitivity to that obtained using observations from two western region SHADOZ locations (Java and Kuala Lumpur) and three eastern region SHADOZ locations (American Samoa, Hilo, and San Cristobal) for 1998–2009. Although in the eastern region only American Samoa is within the box defined by Ziemke *et al.* [2010], the other two locations are just north (Hilo) and east (San Cristobal) of the region and still located in the area significantly correlated with ENSO. We deseasonalized each ozonesonde record prior to averaging them within each region and then regress the resulting values against the Niño 3.4 Index. In the western region (red diamonds), values are nearly all statistically significant and positive (2 standard deviation interval shown from regression). In the eastern region (blue diamonds) SHADOZ reveals significant large negative values in the upper troposphere similar to those simulated. In the low to mid troposphere ozone anomalies are generally not significantly different from zero. Also, plotted on Figure 4 are the ozone sensitivities from the GEOS CCM simulation (solid curves) sampled at the same locations as the SHADOZ stations. In the western region the GEOS CCM simulation underestimates the magnitude of the positive anomalies, while in the upper troposphere of the eastern region the negative anomalies are larger than those derived from SHADOZ stations. Overall these patterns in SHADOZ regional composites are similar to those obtained by Lee *et al.* [2010] for two individual stations (Kuala Lumpur

and San Cristobal), and more recently for several stations used by *Randel and Thompson* [2011].

4. Conclusions

[14] We have demonstrated that the relationship between tropical SST anomalies and the response of tropical tropospheric ozone is clearly reproduced in the GEOS CCM simulation forced with time varying observed SSTs. Such agreement requires both a realistic response of the circulation to the SST and realistic simulated horizontal and vertical ozone gradients. The OEI represents an essential physical relationship that coupled chemistry-climate models should reproduce and is potentially useful in future chemistry-climate model evaluations. Tropical tropospheric ozone changes appear to be congruent with anomalous changes to the Walker circulation cell.

[15] The impact of changes in biomass burning is not considered in this simulation. Although, previous work [e.g., *Thompson et al.*, 2001] has shown its importance in ozone production, time-dependent emissions are not critical for reproducing the OEI. *Ziemke et al.* [2009] used emissions appropriate for the 2006 El Niño event; their results suggest that the change in emissions accounts for no more than 20% of the OEI response. Simulations indicate that ozone anomalies produced from interannual variability in biomass burning are transported throughout the tropics over the 3 month averaging period that is used in constructing the OEI. Only a strong local increase in one region but not the other will impact the OEI.

[16] This analysis demonstrates that ENSO-related changes in the circulation, thermal structure and composition drive tropical ozone variability. Future work will include a detailed budget analysis to determine the relative contributions of dynamical, chemical, and thermal changes to the sensitivity of ozone and related species to ENSO.

[17] **Acknowledgments.** This research was supported by the NASA MAP, ACMAP, and Aura programs. We would like to thank Paul Newman and two anonymous reviewers for some very helpful comments on this paper and Stacey Frith for helping with the model output processing. We also thank those involved in model development at GSFC, and high-performance computing resources provided by NASA's Advanced Supercomputing Division.

[18] The Editor thanks Masaaki Takahashi and an anonymous reviewer for their assistance in evaluating this paper.

References

- Bey, I., D. J. Jacob, R. M. Yantosca, J. A. Logan, B. D. Field, A. M. Fiore, Q. Li, H. Liu, L. J. Mickley, and M. Schultz (2001), Global modeling of tropospheric chemistry with assimilated meteorology: Model description and evaluation, *J. Geophys. Res.*, *106*, 23,073–23,095, doi:10.1029/2001JD000807.
- Bjerknes, J. (1969), Atmospheric teleconnections from the equatorial Pacific, *Mon. Weather Rev.*, *18*, 820–829.
- Chandra, S., et al. (1998), Effects of 1997–1998 El Niño on tropospheric ozone and water vapor, *Geophys. Res. Lett.*, *25*, 3867–3870, doi:10.1029/98GL02695.
- Chandra, S., et al. (2002), Tropical tropospheric ozone: Implications for dynamics and biomass burning, *J. Geophys. Res.*, *107*(D14), 4188, doi:10.1029/2001JD000447.
- Chandra, S., et al. (2009), Effects of the 2006 El Niño on tropospheric ozone and carbon monoxide: Implications for dynamics and biomass burning, *Atmos. Chem. Phys.*, *9*, 4239–4249, doi:10.5194/acp-9-4239-2009.
- Doherty, R. M., D. S. Stevenson, C. E. Johnson, W. J. Collins, and M. G. Sanderson (2006), Tropospheric ozone and El Niño–Southern Oscillation: Influence of atmospheric dynamics, biomass burning emissions, and future climate change, *J. Geophys. Res.*, *111*, D19304, doi:10.1029/2005JD006849.
- Duncan, B. N., S. E. Strahan, Y. Yoshida, S. D. Steenrod, and N. Livesey (2007), Model study of the cross-tropopause transport of biomass burning pollution, *Atmos. Chem. Phys.*, *7*, 3713–3736, doi:10.5194/acp-7-3713-2007.
- Enfield, D. B. (1989), El Niño, past and present, *Rev. Geophys.*, *27*(1), 159–187, doi:10.1029/RG027i001p00159.
- Jacobson, M. Z. (1995), Computation of global photochemistry with SMVGear II, *Atmos. Environ.*, *29*, 2541–2546, doi:10.1016/1352-2310(95)00194-4.
- Kley, D., P. J. Crutzen, H. G. J. Smit, H. Vomel, S. J. Oltmans, H. Grassl, and V. Ramanathan (1996), Observations of near-zero ozone concentrations over the convective Pacific: Effects on air chemistry, *Science*, *274*, 230–233, doi:10.1126/science.274.5285.230.
- Langford, A. O. (1999), Stratosphere-troposphere exchange at the subtropical jet: Contribution to the tropospheric ozone budget at midlatitudes, *Geophys. Res. Lett.*, *26*, 2449–2452, doi:10.1029/1999GL900556.
- Langford, A. O., T. J. O'Leary, C. D. Masters, K. C. Aikin, and M. H. Proffitt (1998), Modulation of middle and upper tropospheric ozone at northern midlatitudes by the El Niño/Southern Oscillation, *Geophys. Res. Lett.*, *25*, 2667–2670, doi:10.1029/98GL01909.
- Lee, S., D. M. Shelow, A. M. Thompson, and S. K. Miller (2010), QBO and ENSO variability in temperature and ozone from SHADOZ, 1998–2005, *J. Geophys. Res.*, *115*, D18105, doi:10.1029/2009JD013320.
- Oort, A. H., and J. J. Yienger (1996), Observed interannual variability in the Hadley circulation and its connection to ENSO, *J. Clim.*, *9*(11), 2751–2767, doi:10.1175/1520-0442(1996)009<2751:OIVITH>2.0.CO;2.
- Philander, S. G. (1989), *El Niño, La Niña, and the Southern Oscillation*, 293 pp., Academic, San Diego, Calif.
- Quan, X.-W., H. F. Diaz, and M. P. Hoerling (2004), Change in the tropical Hadley cell since 1950, in *The Hadley Circulation: Past, Present, and Future*, edited by H. F. Diaz and R. S. Bradley, pp. 85–120, Cambridge Univ. Press, New York, doi:10.1007/978-1-4020-2944-8_3.
- Randel, W. J., and J. B. Cobb (1994), Coherent variations of monthly mean total ozone and lower stratospheric temperature, *J. Geophys. Res.*, *99*, 5433–5447, doi:10.1029/93JD03454.
- Randel, W. J., and A. M. Thompson (2011), Interannual variability and trends in tropical ozone derived from SAGE II satellite data and SHADOZ ozone-sondes, *J. Geophys. Res.*, *116*, D07303, doi:10.1029/2010JD015195.
- Rayner, N. A., D. E. Parker, E. B. Horton, C. K. Folland, L. V. Alexander, D. P. Rowell, E. C. Kent, and A. Kaplan (2003), Global analyses of sea surface temperature, sea ice, and night marine air temperature since the late nineteenth century, *J. Geophys. Res.*, *108*(D14), 4407, doi:10.1029/2002JD002670.
- Rienecker, M. M., et al. (2008), The GEOS-5 data assimilation system—Documentation of versions 5.0.1, 5.1.0, and 5.2.0, in *Technical Report Series on Global Modeling and Data Assimilation*, vol. 27, edited by M. J. Suarez, NASA Tech. Memo. NASA/TM-2008-104606, NASA Goddard Space Flight Cent., Greenbelt, Md.
- Strahan, S. E., B. N. Duncan, and P. Hoor (2007), Observationally-derived diagnostics of transport in the lowermost stratosphere and their application to the GMI chemistry transport model, *Atmos. Chem. Phys.*, *7*, 2435–2445, doi:10.5194/acp-7-2435-2007.
- Sudo, K., and M. Takahashi (2001), Simulation of tropospheric ozone changes during 1997–1998 El Niño: Meteorological impact on tropospheric photochemistry, *Geophys. Res. Lett.*, *28*, 4091–4094, doi:10.1029/2001GL013335.
- Thompson, A. M., et al. (2001), Tropical tropospheric ozone and biomass burning, *Science*, *291*, 2128–2132, doi:10.1126/science.291.5511.2128.
- Thompson, A. M., et al. (2003), Southern Hemisphere Additional Ozone-sondes (SHADOZ) 1998–2000 tropical ozone climatology: 1. Comparison with Total Ozone Mapping Spectrometer (TOMS) and ground-based measurements, *J. Geophys. Res.*, *108*(D2), 8238, doi:10.1029/2001JD000967.
- Voulgarakis, A., P. Hadjinicolaou, and J. A. Pyle (2011), Increases in global tropospheric ozone following an El Niño event: Examining stratospheric ozone variability as a potential driver, *Atmos. Sci. Lett.*, *12*, 228–232, doi:10.1002/asl.318.
- Zeng, G., and J. A. Pyle (2005), Influence of El Niño Southern Oscillation on stratosphere/troposphere exchange and the global tropospheric ozone budget, *Geophys. Res. Lett.*, *32*, L01814, doi:10.1029/2004GL021353.
- Ziemke, J. R., and S. Chandra (2003), La Niña and El Niño-induced variabilities of ozone in the tropical lower atmosphere during 1970–2001, *Geophys. Res. Lett.*, *30*(3), 1142, doi:10.1029/2002GL016387.
- Ziemke, J. R., S. Chandra, B. N. Duncan, L. Froidevaux, P. K. Bhartia, P. F. Levelt, and J. W. Waters (2006), Tropospheric ozone determined from Aura OMI and MLS: Evaluation of measurements and comparison with the Global Modeling Initiative's Chemical Transport Model, *J. Geophys. Res.*, *111*, D19303, doi:10.1029/2006JD007089.
- Ziemke, J. R., S. Chandra, B. N. Duncan, M. R. Schoeberl, O. Torres, M. R. Damon, and P. K. Bhartia (2009), Recent biomass burning in the tropics and related changes in tropospheric ozone, *Geophys. Res. Lett.*, *36*, L15819, doi:10.1029/2009GL039303.

Ziemke, J. R., S. Chandra, L. D. Oman, and P. K. Bhartia (2010), A new ENSO index derived from satellite measurements of column ozone, *Atmos. Chem. Phys.*, *10*, 3711–3721, doi:10.5194/acp-10-3711-2010.

A. R. Douglass, J. E. Nielsen, L. D. Oman, J. M. Rodriguez, and J. R. Ziemke, Atmospheric Chemistry and Dynamics Branch, NASA Goddard

Space Flight Center, Code 613.3, Greenbelt, MD 20771, USA. (luke.d.oman@nasa.gov)

C. Lang and D. W. Waugh, Department of Earth and Planetary Science, Johns Hopkins University, 3400 North Charles St., Baltimore, MD 21218, USA.